

Paclitaxel/Tetrandrine Coloaded Nanoparticles Effectively Promote the Apoptosis of Gastric Cancer Cells Based on “Oxidation Therapy”

Xiaolin Li,^{†,‡,§} Xiaowei Lu,^{‡,§} Huae Xu,^{§,||} Zhenshu Zhu,^{⊥,#} Haitao Yin,[†] Xiaoping Qian,[†] Rutian Li,[†] Xiqun Jiang,[⊥] and Baorui Liu^{*,†}

[†]The Comprehensive Cancer Center of Drum-Tower Hospital, Medical School of Nanjing University & Clinical Cancer Institute of Nanjing University, Nanjing, 210008, P. R. China

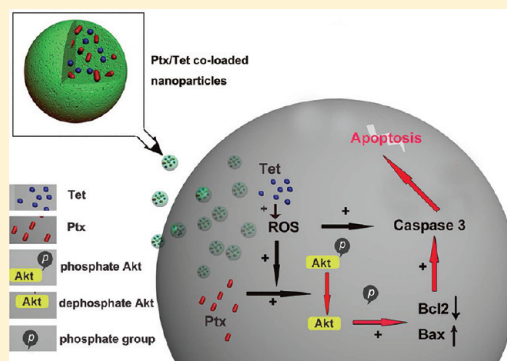
[‡]Department of Geriatrics and ^{||}Department of Pharmacy, the First Affiliated Hospital to Nanjing Medical University, Nanjing, 210029, P. R. China

[⊥]Laboratory of Mesoscopic Chemistry and Department of Polymer Science & Engineering College of Chemistry & Chemical Engineering, Nanjing University, Nanjing, 210093, P. R. China

ABSTRACT: Paclitaxel (Ptx) has demonstrated encouraging activity in the treatment of gastric cancer. Development of drug-containing biodegradable polymeric nanoparticles (np) becomes one of the solutions to relieve side effects of Ptx. However, Ptx-loaded nanoparticles prepared by the nanoprecipitation method are unstable in the aqueous phase. Here we report that tetrandrine (Tet) effectively increases the stability of Ptx-loaded nanoparticles when Tet is coencapsulated with Ptx into mPEG-PCL nanoparticles. The current study demonstrates the synergistic antitumor effect of Tet and Ptx against gastric cancer cells, which provides the basis of coadministration of Tet and Ptx by nanoparticles. It is reported that the cellular chemoresistance to Ptx correlates with intracellular antioxidant capacity and the depletion of cellular antioxidant capacity could enhance the cytotoxicity of Ptx. Tet effectively induces intracellular ROS production.

Therefore, the present study provides a promising novel therapeutic strategy basing on “oxidation therapy” that it could amplify the antitumor effect of paclitaxel by employing Tet as a pro-oxidant. More intracellular Tet accumulation by endocytosis of Ptx/Tet-np than equivalent doses of free drug leads to more intracellular ROS induction, which could efficiently enhance the cytotoxicity of Ptx by sequential inhibition of ROS-dependent Akt pathway and activation of apoptotic pathways, all of which would mediate the superior cytotoxicity of Ptx/Tet-np over free drug. The present results suggest that the codelivery of Ptx and Tet by nanoparticles provides a novel therapeutic strategy basing on “oxidation therapy” against gastric cancer.

KEYWORDS: paclitaxel, tetrandrine, nanoparticle, antitumor, oxidation therapy



1. INTRODUCTION

Paclitaxel (Ptx), one of the most widely used anticancer agent, has demonstrated extraordinary activities against a variety of solid tumors including advanced/recurrent gastric cancer.^{1,2} However, the therapeutic response of Ptx is often associated with severe side effects caused by its nonspecific toxic effects and special solvents (Cremophor EL).^{3,4} Recently biodegradable polymeric nanoparticles (np) composed of amphiphilic copolymers, as promising tumor-targeted drug delivery systems, have attracted intense interest.^{5,6} The characteristic structure of amphiphilic copolymers enables itself to self-assemble into nanoscaled core-shell spherical structures with the hydrophobic drug entrapped in the core and to disperse in the aqueous phase by virtue of a hydrophilic shell. Drug-loaded nanoparticles formed by amphiphilic copolymers exhibit a sustained release manner and can escape from the scavenging of the reticuloendothelial systems (RES) effectively.⁷ Moreover, nanoparticulate drug delivery systems were proved to be preferentially located in the tumor tissue by the enhanced permeability and retention (EPR) effect.⁸

The other hindrance for further application of paclitaxel in the clinic is the emerging resistance by tumor cells. Previous studies reported that accumulation of hydrogen peroxide is an early and crucial step for Ptx-induced cancer cell death both in vitro and in vivo.^{9–12} It was also reported that Ptx chemoresistance correlates very well to intracellular antioxidant capacity. Ptx cytotoxicity can be significantly reduced by an antioxidant such as selenium, while depletion of cellular antioxidant capacity can enhance Ptx cytotoxicity.^{11,13} It is known that the antioxidative defense system is intrinsically high in most cancer cells. The balance between reactive oxygen species (ROS) and cellular antioxidant capacity determines the fate of cells, and overcoming the antioxidative defense systems by accelerating ROS production could promote apoptosis.^{9–13}

Received: May 27, 2011

Revised: December 4, 2011

Accepted: December 15, 2011

Published: December 15, 2011

Therefore, cellular total antioxidant capacity is a critical determinant of cellular sensitivity to Ptx and it is rational to propose the strategy (oxidation therapy) that conquering cellular antioxidant capacity by coadministration of pro-oxidants would enhance the efficacy of Ptx.

Tetrandrine (Tet), a bis-benzylisoquinoline alkaloid isolated from the root of Hang-Fang-Chi (*Stephania tetrandra* S. Moore), had antitumor capacity both in cultured tumor cells and in animal models.^{14,15} Tet can effectively induce oxidative stress leading to elevated intracellular ROS, eventually resulting in the apoptosis of tumor cells.^{16,17} Results from our lab showed that Tet significantly enhanced the cytotoxicity of docetaxel, and its possible mechanism might be the synergistic apoptotic effect.¹⁸ However, the application of Tet is restricted by the limited water solubility and low bioavailability caused by its physical properties. It is reported in our previous report that higher uptake efficiency, more ROS generation, and stronger activation of the ROS-dependent apoptotic pathway were induced by an equivalent dose of Tet delivered by nanoparticles.¹⁹

Our preliminary study showed that Ptx-loaded nanoparticles prepared by the nanoprecipitation method are unstable in the aqueous phase, while Tet could effectively stabilize Ptx-loaded nanoparticles with the coencapsulation of Tet and Ptx. Moreover, the synergistic antitumor effect of Tet and Ptx against cancer cells provides the basis of coadministration of Tet and Ptx for cancer therapy.

The purpose of the present study is to provide a novel therapeutic strategy basing on "oxidation therapy" that could amplify the antitumor effect of Ptx by employing Tet as a pro-oxidant. This novel approach utilizes polymeric nanoparticles as drug carriers to codeliver lipophilic Ptx and Tet for optimal therapeutic efficacy. In the present study, we prepared biodegradable core-shell mPEG-PCL nanoparticles containing Ptx and Tet simultaneously and examined the in vitro efficacy in gastric cancer cell line.

2. EXPERIMENTAL SECTION

2.1. Materials. Paclitaxel (Ptx) and tetrandrine (Tet) were kindly provided by Zhejiang Haizheng Pharmaceutical Co. Ltd. According to our previous work,^{19,20} PCL20k-PEG4k nanoparticles were applied in the following procedure for their higher drug loading content and encapsulation efficiency. 3-(4,5-Dimethylthiazol-2-yl)-2,5-diphenyltetrazolium bromide (MTT) and 2,7-dichlorofluorescein diacetate (H₂DCF-DA) were purchased from Sigma Chemical Co. (St. Louis, MO, U.S.A.). All other chemicals were of analytical grade and used without further purification.

Human low-differentiated gastric adenocarcinoma cell line BGC-823 was obtained from Shanghai Institute of Cell Biology (Shanghai, China). Cells were cultured in RPMI 1640 medium with 10% fetal bovine serum and 100 U/mL penicillin-streptomycin at 37 °C in a water-saturated atmosphere with 5% CO₂.

2.2. Methods. **2.2.1. Formulation of Nanoparticles.** Ptx/Tet coloaded nanoparticles were prepared by a nanoprecipitation method as described previously with minor modification.^{19,20} Briefly, 10 mg of mPEG-PCL block copolymers and a predetermined amount of Tet and Ptx were dissolved in an aliquot of acetone. The obtained organic solution was added dropwise into 10× volumes of distilled water under gentle stirring at room temperature. The solution was dialyzed in a dialysis bag (MWCO 12000) to remove acetone thoroughly. The resulting bluish aqueous solution was filtered through a

0.22 μm filter membrane to remove nonincorporated drugs and copolymer aggregates. Coumarin-6 loaded Ptx/Tet nanoparticles were prepared by adding coumarin-6. Drug-free nanoparticles were produced in a similar way by eliminating drugs. Solutions of drug-loaded nanoparticles and empty nanoparticles were then lyophilized for further utilization.

2.2.2. Characterization of Nanoparticles. Atomic force microscopy (AFM, SPI3800, Seiko Instruments, Japan) and transmission electron microscope (TEM, JEM-100S Japan) were used to visualize nanoparticles.^{19,20} Mean diameter and size distribution were measured before lyophilization by photon correlation spectroscopy (DLS) using a Brookhaven BI-9000AT instrument (Brookhaven Instruments Corporation, NY, USA). Zeta potential was measured by the laser Doppler anemometry (Zeta Plus, Zeta Potential Analyzer, Brookhaven Instruments Corporation, NY, USA).

2.2.3. Drug Loading Content (DLC) and Encapsulation Efficiency (EE). The concentrations of Ptx and Tet were assayed on a Shimadzu LC-10AD (Shimadzu, Japan) HPLC system equipped with a Shimadzu UV detector and an Agilent C-18, 5 μm, 200 mm × 4.6 mm RP-HPLC analytical column. The mobile phase for Tet consisted of methanol (spectral grade, Merck, Germany)/double-distilled water/ethylamine (90/10/0.05, v/v/v) pumped at a flow rate of 1.0 mL/min with determination wavelength of 282 nm. The concentration of Tet was determined based on the peak area at the retention time of 4.83 min by reference to a calibration curve.

The mobile phase for detecting Ptx consisted of acetonitrile (spectral grade, Merck, Germany)/double-distilled water (58/42, v/v) pumped at a flow rate of 1.0 mL/min with determination wavelength of 228 nm. The concentration of Ptx was determined based on the peak area at the retention time of 7.3 min by reference to a calibration curve.

The following equations were applied to calculate the drug loading content (eq 1) and encapsulation efficiency (eq 2).

drug loading content (%)

$$= \text{wt of the drug in nanoparticles} / \text{wt of the nanoparticles} \times 100\% \quad (1)$$

encapsulation efficiency (%)

$$= \text{wt of the drug in nanoparticles} / \text{wt of the feeding drugs} \times 100\% \quad (2)$$

2.2.4. In Vitro Release of Ptx/Tet Coloaded Nanoparticles. For in vitro release detection, 10 mg of lyophilized Ptx/Tet coloaded nanoparticles were suspended in 1 mL of 0.1 M phosphate buffered saline (PBS, pH 7.4). The solution was then placed into a preswelled dialysis bag with a 12 kDa molecular weight cutoff (Sigma) and immersed into 20 mL of 0.1 mol/L PBS, pH 7.4, at 37 °C with gentle agitation. One milliliter samples were withdrawn from the incubation medium and measured for Tet and Ptx concentrations as described above. After sampling, an equal volume of fresh PBS was immediately added into the incubation medium. The concentration of Tet or Ptx released from the nanoparticles was expressed as a percentage of the total Tet or Ptx in the nanoparticles and plotted as a function of time respectively.

2.2.5. Nanoparticle Uptake by BGC823 Cells. Coumarin-6 was utilized as fluorescent marker to assess the efficiency of nanoparticle uptake by tumor cells. About 5×10^5 BGC823 cells were seeded in 6-well plates with RPMI 1640 supplemented with 10% fetal bovine serum and allowed to adhere at 37 °C with 5% CO₂ for 24 h prior to the assay. The medium was then replaced with 10 mL of fresh RPMI 1640 containing

coumarin-6 loaded nanoparticles (indicated by dose of coumarin-6). After 4 h incubation, the cell monolayers were rinsed three times with PBS buffer to remove excess nanoparticles. The cells were viewed and imaged under a fluorescence microscope (Carl Zeiss, Goettingen, Germany) using a FITC filter.

2.2.6. *In Vitro* Cytotoxicity Studies. Drugs were added with six different concentrations of the single agent and six different concentrations of both agents at their fixed ratio based on their respective individual IC₅₀ values for 48 h. The fractional inhibition of cell proliferation was calculated by comparison to control cultures. Dose–response curves were obtained for each drug, and for multiple dilutions of a fixed-ratio combination of the two drugs. Median effect analysis using the combination index (CI) method of Chou and Talalay²¹ was employed to determine the nature of the interaction observed between Tet and Ptx.

The CI is defined by the following equation: $CI = (D)_1 / (Dx)_1 + (D)_2 / (Dx)_2 + \alpha(D)_1(D)_2 / (Dx)_1(Dx)_2$, in which (D)₁ and (D)₂ are the concentrations for D1 (Tet) and D2 (Ptx) alone that gives $x\%$ inhibition, whereas (D)₁ and (D)₂ in the numerators are the concentrations of Tet and Ptx that produce the identical level of effect in combination. $\alpha = 0$ when the drugs are mutually exclusive (i.e., with similar modes of action), while $\alpha = 1$ if they are mutually nonexclusive (i.e., with independent modes of action). $CI > 1$ indicates antagonism, $CI < 1$ indicates synergy, and $CI = 1$ indicates additivity. The CI ratio represented here is the mean value derived from at least three independent experiments.

The *in vitro* drug-induced cytotoxic effects were measured by the MTT reduction assay.²² For the cooperative assessment, cells were exposed to a series of doses of free Tet alone, free Ptx alone, and Ptx/Tet-np, with DMSO treatment (concentration < 0.1%) as negative control at 37 °C. After treatment, 1/10 volume of MTT was added to each well, and the plate was further incubated at 37 °C for another 4 h. Two hundred microliters of DMSO was added to each well to solubilize the MTT–formazan product after removal of the medium. Absorbance at 570 nm was measured with a multiwell spectrophotometer (BioTek, Winooski, VT, USA). Growth inhibition was calculated as a percentage of the untreated controls, which were not exposed to drugs.

2.2.7. Detection of Intracellular ROS. In this section, the doses of Ptx and Tet were determined at 0.05 μ M and 10 μ M, respectively, according to IC₅₀ values of Ptx and Tet on BGC823 cells calculated from MTT analysis. H₂DCF-DA was used to detect intracellular generation of ROS by modification.^{9–11} Briefly, BGC823 cells (2×10^5) were cultured with Ptx, Tet, Ptx-np or Ptx/Tet-np, with VitE (10 μ M) as the antioxidant. After 48 h incubation, cells were incubated with 5 mM H₂DCF-DA for 30 min. After washing three times with cold PBS, the intensity of fluorescence was determined by a fluorescence spectrophotometer under an emission wavelength of 535 nm with an excitation wavelength of 485 nm. The obtained values were expressed as folds of the controls. According to green fluorescence of DCF, typical images of intracellular ROS generation were obtained. The lighter the fluorescence is, the greater the ROS generation is.

2.2.8. Western-Blot Analysis. BGC-823 cells were cultured under the same conditions as in the *in vitro* ROS studies. The concentrations of Ptx and Tet were set at 0.05 μ M and 10 μ M, respectively. Protein levels of Akt, p-Akt, Procaspase3, Bcl-2 and Bax were analyzed by Western blot. Briefly, cell lysates were prepared, electrotransferred, and then immunoblotted

with anti-Akt (Santa Cruz Biotechnology), anti-phospho-Akt (Sigma, USA), anti-procaspase3, anti-Bcl-2 and anti-Bax (Santa Cruz Biotechnology). For phospho-protein detection, cells were washed with ice-cold PBS containing 1 mM Na₃VO₄ and 1 mM NaF, and lysed in a buffer (20 mM Tris–Cl (pH 8.0), 137 mM NaCl, 10% glycerol, 1% Triton X-100, 1 mM Na₃VO₄, 1 mM NaF, 2 mM EDTA, 200 nM aprotinin, 20 mM leupeptin, 50 mM phenanthroline, 280 mM benzamidine-HCl). Detection was performed with Western blotting reagent ECL (Amersham), and chemiluminescence was exposed by the filters of Kodak X-Omat films.

2.2.9. Caspase-3 Activity Analysis. BGC-823 cells were cultured under the same conditions as in the Western-blot analysis. Determination of caspase-3 activity was performed by the caspase colorimetric protease assay kit (Keygen Biotech, Nanjing, China) by following the manufacturer's instruction. The optical density was measure at 405 nm. The obtained values were expressed as folds of controls.

2.2.10. Statistical Analysis. Data were expressed as the mean \pm SD of three independent experiments. Statistical analysis for the comparison of relative groups was based on Student's *t* test or ANOVA analysis. Significance was accepted at the 0.05 level of probability.

3. RESULTS

3.1. Fabrication and Characterization of mPEG-PCL Nanoparticles. The relative characteristics of the mPET-PCL polymers were reported in previous studies.^{19,20} Different phenomena could be noticed in the preparation of Ptx-np and Ptx/Tet-np. Ptx-np were highly unstable when acetone was removed during the dialysis process. In the following 2 h, large amount of precipitates were observed. On the contrary, Ptx/Tet-np remained stable in the following two weeks at room temperature (Figure 1A). With time going on, the size of Ptx/Tet-np showed less variation during two weeks, which suggested the satisfied stability of Ptx/Tet-np (Figure 1C). The morphological images of the Ptx/Tet-np obtained from AFM (Figure 1B2) and TEM (Figure 1B1; 1B3) indicated that the nanoparticles, less than 100 nm in size, were spherical in shape with a smooth surface, which was in accordance with the DLS measurement presented in our previous report.^{19,20} Figure 1B1 shows the images of Ptx/Tet-np without freeze-drying while Figure 1B3 was the photograph of the freeze-dried Ptx/Tet-np. The diameter of Ptx/Tet-np after freeze-drying was slightly larger than that before freeze-drying as indicated in Table 1. In addition, the zeta potential of freeze-dried Ptx/Tet-np showed no obvious alteration when compared with the non-freeze-dried nanoparticles (Table 1). Therefore, it demonstrated that Poloxamer 188, a selected freeze-drying protector, could effectively prevent Ptx/Tet-np from aggregation after freeze-drying.

3.2. Drug Loading, Encapsulation Efficiency and State of the Drug Incorporated in the Nanoparticles. Table 1 showed the drug loading content and encapsulation efficiency of Ptx/Tet-np. By varying the feeding ratio of copolymer and drugs, the highest drug loading content of Ptx and Tet was $13.1 \pm 0.4\%$ and $15.4 \pm 0.6\%$ with the encapsulation efficiency being $82.4 \pm 5.5\%$ and $87.3 \pm 6.2\%$ respectively.

3.3. In Vitro Release Pattern of Ptx/Tet-np. Figure 1D shows the sustained release profile of Ptx/Tet-np. An initial burst in the release pattern of Ptx or Tet indicated that the affiliation of certain drugs to the surface of the nanoparticles was unavoidable. In the following period, release of Ptx or Tet was observed in a sustained manner from the core–shell

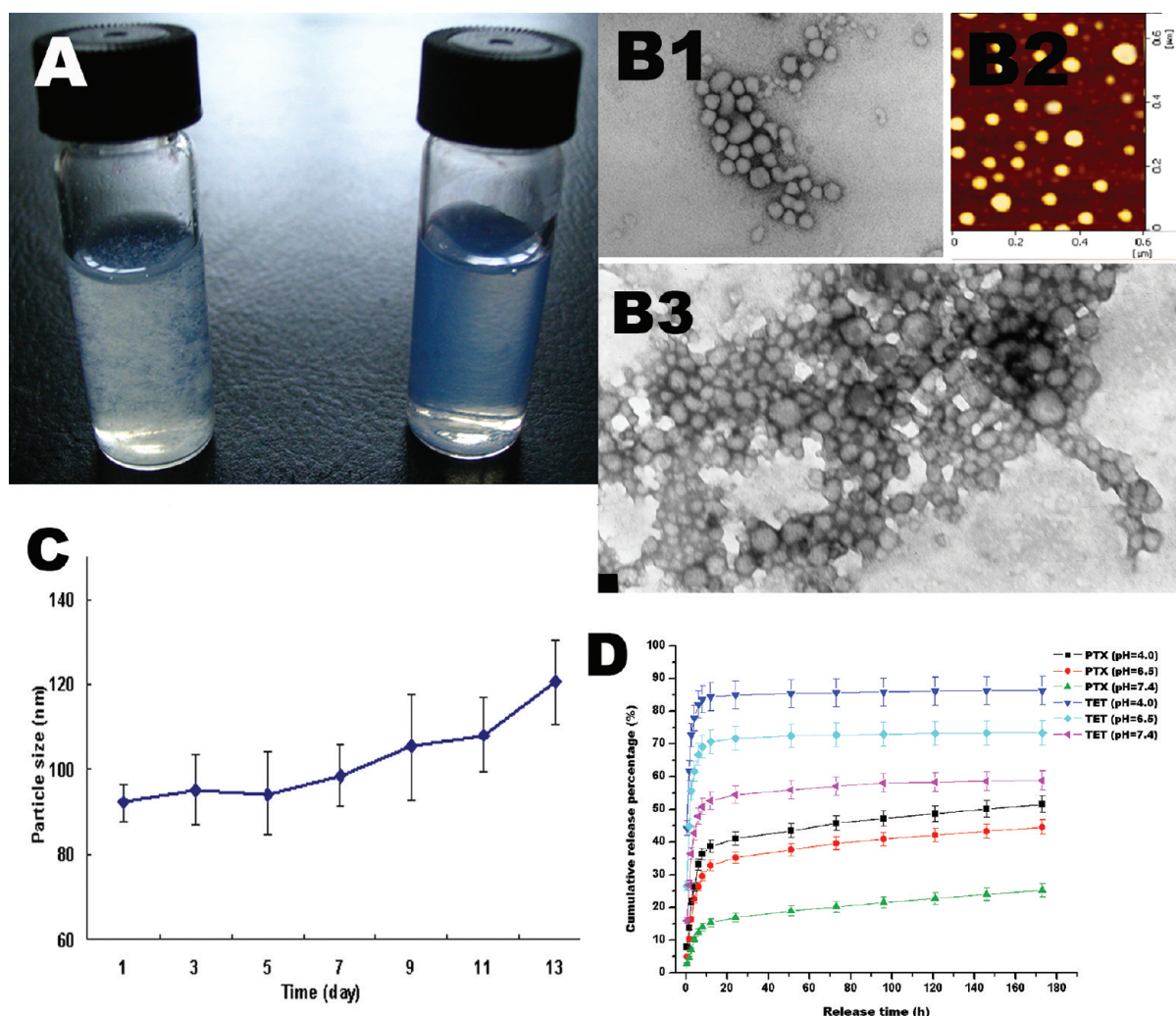


Figure 1. Characterization of Ptx/Tet-np. A: pictures of Ptx-np and Ptx/Tet-np at routine temperature. (Left: Ptx-np. Right: Ptx/Tet-np.) B1: TEM image of Ptx/Tet-np (before lyophilized). B2: AFM image of Ptx/Tet-np (before lyophilized). B3: TEM image of Ptx/Tet-np (after lyophilized). C: Size change of Ptx/Tet-np at routine temperature during 2 weeks. D: In vitro release kinetics of Ptx/Tet-np with different pHs at routine temperature.

Table 1. Mean Particle Size and Drug Load Efficiency of Two Kinds of Nanoparticles

| np | mean particle size (nm) ^a | polydispersity | zeta potential (mV) | DLC ^b (%) | | EE ^c (%) | |
|------------|--------------------------------------|----------------|---------------------|----------------------|-----------------|---------------------|-----------------|
| empty np | 72.3 ± 0.7 | 0.13 ± 0.06 | −5.3 ± 0.9 | na | | na | |
| Ptx/Tet-np | 77.2 ± 1.9 | 0.14 ± 0.09 | −6.6 ± 2.1 | 13.1 ± 0.4(Ptx) | 15.4 ± 0.6(Tet) | 82.4 ± 5.5(Ptx) | 87.3 ± 6.2(Tet) |

^aThe SD value was for the mean particle size obtained from the three measurements of a single batch. ^bDLC = drug loading content. ^cEE = encapsulation efficiency.

nanoparticles as shown in Figure 1D. Most importantly, both Ptx and Tet displayed a pH-dependent release profile. With the decrease of pH values from 7.4 to 4.0, the release percents of Ptx or Tet increased obviously. For instance, in the first 5 h, less than 50% of Tet was released at a pH of 7.4 while more than 80% was detected in the release medium at a pH of 4.0.

3.4. Cellular Uptake of Nanoparticles. The hydrophobic fluorescent agent, coumarin-6, was loaded as a model drug into nanoparticles to explore the uptake efficiency of cancer cells. Two hour incubation with BGC-823 cells was sufficient for the nanoparticles to enter the cells. Coumarin-6 loaded nanoparticles were mostly localized around the nuclei in the cytoplasm (Figure 2).

3.5. Synergistic Anticancer Efficacy of Ptx/Tet-np against BGC-823 Cells. Blank nanoparticles were demonstrated to be nearly nontoxic to BGC-823 cells with the

inhibition rate less than 10% even at a high concentration of 400 $\mu\text{g/mL}$ (data not shown). As shown in Figure 3A, Tet, Ptx and Ptx/Tet-np had dose-response effects against BGC823 cells. Drug combinations delivered by nanoparticles gave a greater decrease of cell survival at each dose. To fully evaluate the nature of the interaction between Tet and Ptx, we analyzed the combination of both drugs using median-effect analysis, which resolved the degree of synergy, additivity, or antagonism at a series of doses. Figure 3B also illustrates the multiple drug effect obtained for BGC-823 cells, which were treated with Tet/Ptx-np and represented as fractional cell growth inhibition (FA) as a function of the CI. The combination of two drugs administered by nanoparticles generated more cell deaths than either of the drugs used singly. For example, an inhibition rate of nearly 50% was detected when exposed to Ptx/Tet-np at a

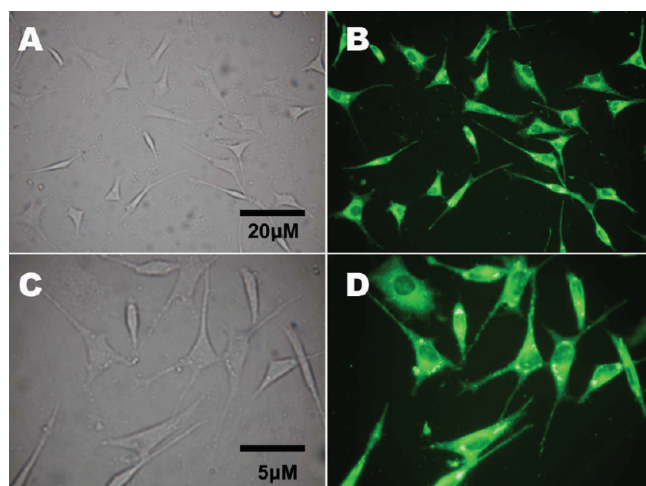


Figure 2. Uptake of fluorescent Ptx/Tet-np by BGC823 cells. A–D: Microscopic images of BGC823 cells incubated with coumarin-6 loaded Ptx/Tet-np for 2 h (A, C, bright field; B, D, fluorescent fields).

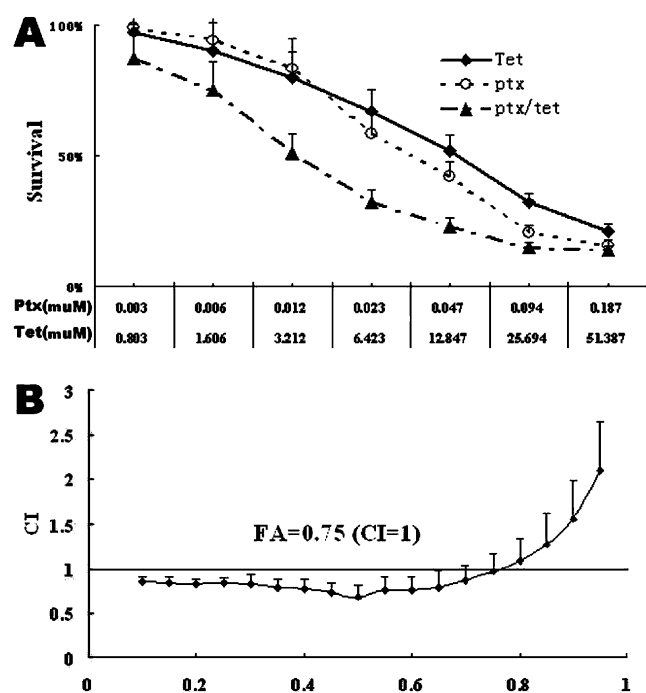


Figure 3. Analysis of synergy between Tet and Ptx for BGC-823 cells by the method of Chou and Talalay.²¹ A: Dose–response curves of Tet, Ptx and Ptx/Tet-np in BGC-823 cells. B: CI values at different levels of growth inhibition effect (fraction affected, FA). Values represents mean \pm SD ($n = 3$).

dose of 3.212 μ M (Tet) and 0.012 μ M (Ptx), while an inhibition rate of less than 20% was observed when cells were treated by the same dose of free Tet or Ptx, respectively. Moreover, median-effect analysis showed that the CI values were below 1 when FA was below 0.75, indicating a synergistic antiproliferative effect of Tet and Ptx in coloaded nanoparticles.

3.6. Ptx/Tet-np Showed High Cytotoxicity and Intracellular ROS Levels, Which Were Resistant to Vitamin E Pretreatment. As shown in Figure 4B, pretreatment of 10 μ M vitamin E for 2 h significantly protected BGC-823 cells from the cytotoxicity of Tet, Ptx or Ptx-np. Most importantly, Ptx/Tet-np induced significantly more cell deaths than other agents

($p < 0.05$) without the pretreatment of vitamin E. However, there was no significant difference between the cytotoxicity of Ptx/Tet-np with and without the pretreatment of 10 μ M vitamin E. For example, when exposed to Ptx/Tet-np without the pretreatment of vitamin E, 20.1% cells survived while 25% cells stayed alive with the pretreatment of vitamin E. It suggested that the pretreatment of vitamin E could hardly protect BGC-823 cells from the cytotoxicity of Ptx/Tet-np.

As shown in Figure 4A,C, empty nanoparticles had no influence on the intracellular ROS levels. Total intracellular ROS levels elevated in cells treated with either free Ptx or Ptx-np. Vitamin E partially reversed the elevation of ROS levels in the cells treated by free Ptx and Ptx-np, there was no difference observed in the production of ROS between the cells exposed to free Ptx and Ptx-np regardless of vitamin E. ROS production in Tet-treated cells is much higher than that in control group ($p < 0.05$), while pretreatment of 10 μ M vitamin E significantly decreases the ROS level induced by Tet ($p < 0.05$). However, it reaches our expectation that, no matter with or without pretreatment of vitamin E, the codelivery of Tet and Ptx in nanoparticles triggered a significantly more ROS production in the cells compared to Ptx or Ptx-np ($p < 0.05$). The induction of intracellular ROS by Ptx/Tet co-np showed more resistance to antioxidant vitamin E, which paralleled the effect of vitamin E on the cytotoxicity of Ptx/Tet-np.

3.7. Ptx/Tet-Loaded Nanoparticles Repressed Akt Activation. In the present study, we found that Ptx or Ptx-np repressed the expression of activated form of Akt (phosphate-Akt, p-Akt) while vitamin E could reverse this alteration in BGC823 cells (Figure 5A), which paralleled the change of ROS and cytotoxicity (Figure 4). By introducing Tet into Ptx-loaded nanoparticles containing both Ptx (0.05 μ M) and Tet (10 μ M), more Akt repression were achieved which were in accordance with higher ROS level and cell apoptosis. Furthermore, Ptx and Tet cocapsulated in nanoparticles significantly inhibited Akt activation regardless of vitamin E.

3.8. Ptx/Tet-Loaded Nanoparticles Downregulated Bcl-2, Upregulated Bax and Induced More Caspase-3 Activation. Here, we studied the expression of Bcl2, Bax, procaspase3 and the activity of caspase-3 in BGC cells treated with Ptx, Ptx-np or Ptx/Tet-np. After treating for 48 h, all of them resulted in a decrease of the inactive pro form of caspase-3 (procaspase-3), a decrease of Bcl2 and an increase of Bax. In our experiments, Ptx/Tet-np led to more decrease of the inactive procaspase-3, more decrease of Bcl2 and more increase of Bax than the equivalent dose of free Ptx or Ptx-np did (Figure 5B).

To quantify the activity of caspase-3, we performed an in vitro assay as shown in Figure 5C. When compared to control, treatment with Ptx, Ptx-np or Ptx/Tet-np for 48 h significantly activated caspase-3 ($p < 0.05$) with about 8-fold increase, 7.5-fold increase and 14-fold increase of caspase-3 activity, respectively. Obviously, Ptx/Tet-np statistically surpassed Ptx and Ptx-np in activating apoptosis.

4. DISCUSSION AND CONCLUSION

In our previous study, we have developed PEG-PCL nanoparticles containing several kinds of anticancer drugs such as resveratrol, Tet, Ptx, cisplatin and curcumin.^{19,20,23,24} The instability of Ptx-np in the aqueous phase has bothered us for a long time. We attempted to develop Ptx/Tet, Ptx/Res coloaded nanoparticles and were surprised to find that Ptx/Tet coloaded nanoparticles could suspend stably in PBS up to one week.

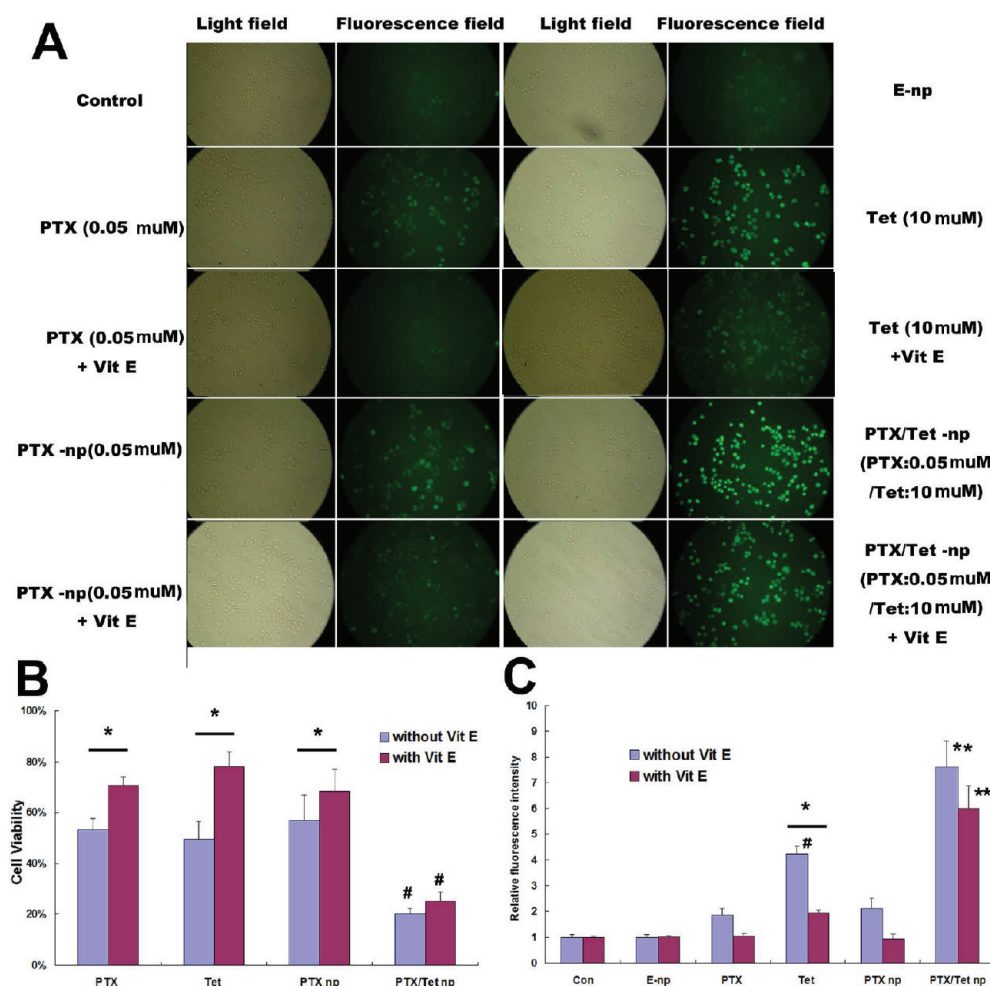


Figure 4. Intracellular ROS levels induced by Ptx/Tet-np and the influence of vitamin E on the induction. A: The DCF fluorescent images of BGC823 cells treated with different agents. B: Influences of vitamin E pretreatment on the cytotoxicity of different agents at an equivalent dose of 10 μ M. Values represents mean \pm SD ($n = 3$). (*) represents $p < 0.05$; (#) represents $p < 0.05$ vs the group treated with Ptx, Tet, or Ptx-np, respectively with or without the pretreatment of vitamin E. C: Intracellular DCF fluorescence intensity of BGC823 cells treated with different agents. All of the values were from the images recorded by fluorescent microscopic images. Values represents mean \pm SD ($n = 3$). (*) represents $p < 0.05$, (#) represents $p < 0.05$ vs control, (**) represents $p < 0.01$ vs control with or without the pretreatment of vitamin E.

Furthermore, the application of freeze-drying not only provides an ideal way to store the drug-loaded nanoparticles but also retains its physicochemical characteristics. The high loading efficiency depends mainly on the hydrophobicity of Ptx or Tet and their satisfying affinity to the hydrophobic core (PCL). The characteristic pH dependent release patterns of Ptx and Tet enable the targeted release of the drugs from the nanoparticles at tumor site because tumor tissues possess a slightly acidic circumstance (pH 6.4). Therefore, the release data indicate that Ptx and Tet can be well released from the core-shell structure of co-loaded polymeric nanoparticles and Ptx/Tet-np might be useful as a controlled release system for cancer therapy.

Although Ptx is a practicable anticancer drug, the hindrance for satisfying chemotherapy is the drug resistance of cancer cells. It is in urgent need to develop promising chemosensitizing strategies, and the combination of several anticancer drugs is a proved strategy of effective therapy. The current report demonstrates the potential of Tet as a chemotherapeutic enhancer for Ptx. Moreover, encapsulation of Tet and Ptx into nanoparticles not only shows better stability than Ptx-loaded nanoparticles but also retains the synergistic anticancer efficiency of Tet and Ptx.

Recent studies reported that treatment with antioxidant partially reversed Ptx inducing cytotoxicity in many kinds of tumor cells.^{9–11} Since higher metabolic rate, more accelerating growing curve and worse circumstance made tumor cells develop stronger antioxidative system to survive, the induction of intracellular ROS generation by certain drugs would optimize the cytotoxicity of Ptx. Earlier reports suggested that ROS play a crucial role in Tet induced apoptosis and cytotoxicity.¹⁶ Overproduction of intracellular ROS is one of the mechanisms involved in chemotherapeutic drug mediated apoptosis of cancer cells.^{25,26} To study whether intracellular ROS play an important role in the synergistic antitumor efficacy of nanoparticle-based delivery of Ptx and Tet, we detected the intracellular ROS levels of cells exposed to different agents by fluorescent microscopy. Significant ROS generation was detected in cells treated with Ptx/Tet-np, which was greater than with Ptx, Ptx-np or Tet alone. It was noted that Tet treatment induced midhigh ROS level in cells and vitamin E obviously diminished the ROS production. However, the highest intracellular ROS level induced by successful codelivery of Ptx and Tet in polymeric nanoparticles was only slightly attenuated by vitamin E. The so-called Trojan strategy of

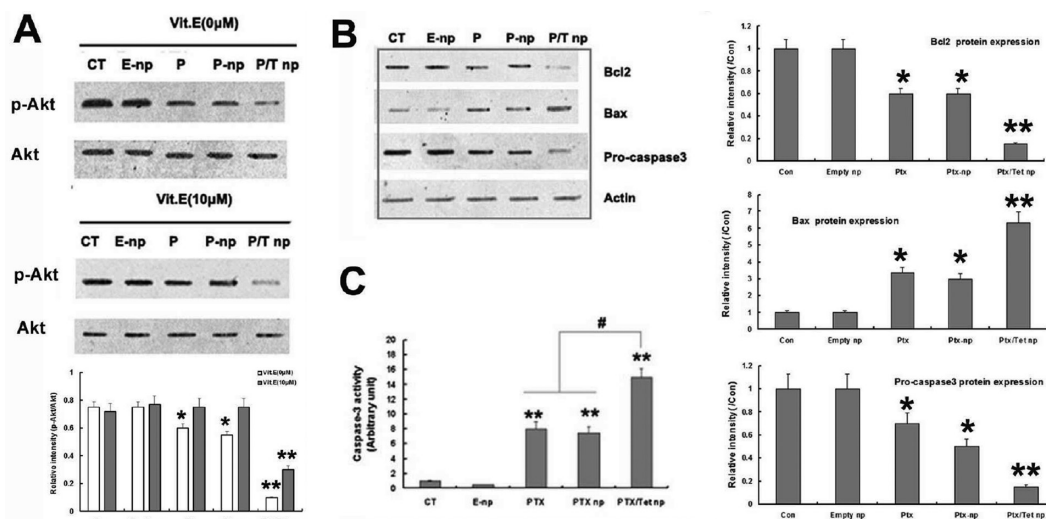


Figure 5. Effects of Ptx/Tet-np on the expression of Akt pathway and apoptotic proteins in BGC823 cells. BGC823 cells were exposed to empty np (E-np), Ptx alone (P), Ptx-np (P-np), or Ptx/Tet-np (P/T-np), respectively. (A) Western blot analysis of p-Akt and Akt. Upper panel: the expression p-Akt and Akt proteins in cells exposed to different agents without the pretreatment of vitamin E. Middle panel: the expression p-Akt and Akt proteins in cells exposed to different agents with the pretreatment of vitamin E (10 μ M). Lower panel: semiquantitative analysis of protein expressions in different groups. (B) Western blot analysis of Bcl-2, Bax, and procaspase-3 in cells exposed to different agents. Right: semiquantitative analysis of Bcl-2, Bax, and procaspase-3 expressions in different groups. (C) Activation analysis of caspase-3. Values represents Mean \pm SD. ** represents $p < 0.01$ vs control. # represents $p < 0.05$.

cellular uptake of nanoparticles by endocytosis can explain this phenomenon.¹⁹ Together with the paralleled MTT assessments that Ptx/Tet-np led to most cell inhibition and that pretreatment with vitamin E protected BGC-823 cells from the cytotoxicity of both free drugs and Ptx-loaded nanoparticles but little reduced the cytotoxicity of Ptx/Tet-np, the above suggested that codelivery of Ptx and Tet in polymeric nanoparticles could effectively induce ROS production and inhibit the viability of gastric cancer cells.

Previous studies indicated that alterations in the PI3k/Akt signal pathway could modulate sensitivity to cancer chemotherapy.^{27,28} Overexpression of Akt decreases paclitaxel-induced apoptosis in ovarian cancer cells.^{29,30} It is crucial for Ptx-based chemotherapy that Ptx inhibits Akt signal and leads to apoptosis. However, ROS was another important messenger modulating Ptx-related tumor apoptosis.^{9,16,26} Recent evidence showed that antioxidant could relieve Ptx induced cytotoxicity and the underlying mechanism was associated with cellular total antioxidative capacity in numerous cancer cells.^{9–11,27,28} Here in the current report we demonstrated that delivery of Ptx by nanoparticles could induce intracellular ROS generation and suppress the activation of Akt pathway, which could be reversed by the pretreatment of vitamin E. On the contrary, codelivery of Tet and Ptx by nanoparticles induced more ROS followed by the significantly lower activation of Akt, with the resistance to vitamin E pretreatment. Therefore, the possible mechanism of the synergistic antitumor effect of Tet and Ptx is through the induction of intracellular ROS and the suppression of the downstream Akt pathway. This effect could be reversed by antioxidant (vitamin E), however, we here suggested that delivery of the two drugs by nanoparticles could significantly enhance the cytotoxicity than free drugs. Additionally, the following ROS generation and Akt suppression by drug-loaded nanoparticles elucidate the mechanisms of the superiority of drug combination nanodelivery system over free drugs.

Intracellular ROS accumulation and sequential Akt pathway inactivation can trigger the apoptotic cascade.³¹ It is known that Bcl-2 exerts a protective effect against apoptosis. Previous studies

have shown that paclitaxel-induced apoptosis in gastric cancer cells is mediated by downregulation of the antiapoptotic gene Bcl-2 and by upregulation of the proapoptotic gene Bax and the activation of caspase-3 is important for tumor cell death.^{31,32} Here we demonstrated that Tet enhanced apoptotic cascades in Ptx treated cancer cells and this effect could be amplified by a nanodrug delivery system.

The current study reported a simple reproducible way to efficiently develop stable controlled releasing Ptx/Tet coloaded nanoparticles by amphiphilic mPEG-PCL block copolymers. Ptx/Tet-np led to more intracellular ROS accumulation, more diminution of p-Akt, and sequential stronger activation of apoptosis, which were resistant to vitamin E (Figure 6). As for

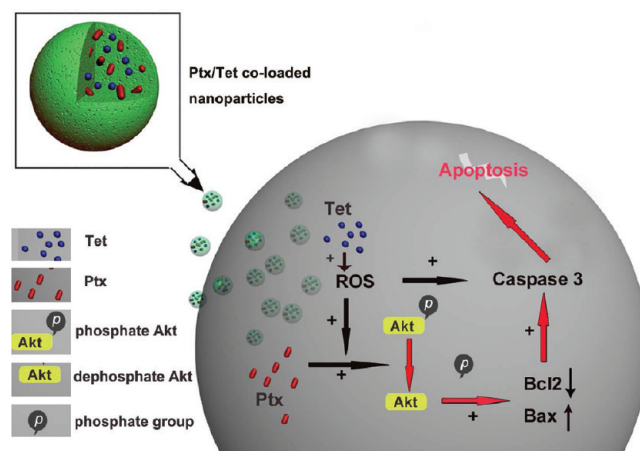


Figure 6. The Trojan strategy of nanoparticle-based Ptx/Tet delivery can effectively lead to higher cell death. More intracellular Tet accumulation by endocytosis of Ptx/Tet-np than equivalent doses of free drug led to more intracellular ROS induction, which could efficiently enhance the cytotoxicity of Ptx by sequential inhibition of ROS-dependent Akt pathway and activation of apoptotic pathways, all of which would mediate the superior cytotoxicity of Ptx/Tet-np over free drug.

the heavy redox balance system in tumor cells, the codelivery of Ptx and Tet by nanoparticles based on “oxidation strategy” may generate more promising outcomes in cancer therapy. Undoubtedly, however, the combinative strategy of “oxidation therapy” by developing Ptx/Tet-containing nanoscale delivery system warrants further research in vivo.

AUTHOR INFORMATION

Corresponding Author

*Drum-Tower Hospital, Medical School of Nanjing University, The Comprehensive Cancer Center, 321 Zhongshan Road, Nanjing, Jiangsu, 210008, P. R. China. Tel: +86-25-83107081. Fax: +86-25-83107081. E-mail: baoruiliu@nju.edu.cn.

Author Contributions

[§]These authors contributed equally to this work.

Present Addresses

[#]Department of Pharmaceutical Analysis, China Pharmaceutical University, Nanjing 210009, P. R. China.

ACKNOWLEDGMENTS

This work was supported by the National Natural Science Foundation of China (NO. 81001077 to X. Li; 81101902 to H. X.; 81100858 to X. Lu; 30872471 to B. L.).

REFERENCES

- (1) Sakamoto, J.; Matsui, T.; Koda, Y. Paclitaxel chemotherapy for the treatment of gastric cancer. *Gastric Cancer* **2009**, *12*, 69–78.
- (2) Woodward, E. J.; Twelves, C. Scheduling of taxanes: a review. *Curr. Clin. Pharmacol.* **2010**, *5*, 226–231.
- (3) Dorr, R. T. Pharmacology and toxicology of Cremophor EL diluent. *Ann. Pharmacother.* **1994**, *28*, S11–S14.
- (4) Bissery, M. C.; Nohynek, G.; Sanderink, G. J.; Lavelle, F. Docetaxel (Taxotere): A review of preclinical and clinical experience. Part I: Preclinical experience. *Anticancer Drugs* **1995**, *6*, 339–355, 363–368.
- (5) Wei, X.; Gong, C.; Gou, M.; Fu, S.; Guo, Q.; Shi, S.; Luo, F.; Guo, G.; Qiu, L.; Qian, Z. Biodegradable poly(epsilon-caprolactone)-poly(ethylene glycol) copolymers as drug delivery system. *Int. J. Pharm.* **2009**, *381*, 1–18.
- (6) van Vlerken, L. E.; Vyas, T. K.; Amiji, M. M. Poly(ethylene glycol)-modified nanocarriers for tumor-targeted and intracellular delivery. *Pharm. Res.* **2007**, *24*, 1405–1414.
- (7) Uhrich, K. E.; Cannizzaro, S. M.; Langer, R. S.; Shakesheff, K. M. Polymeric systems for controlled drug release. *Chem. Rev.* **1999**, *99*, 3181–3198.
- (8) Jain, R. K.; Stylianopoulos, T. Delivering nanomedicine to solid tumors. *Nat. Rev. Clin. Oncol.* **2010**, *7*, 653–664.
- (9) Laurent, A.; Nicco, C.; Chéreau, C.; Goulvestre, C.; Alexandre, J.; Alves, A.; Lévy, E.; Goldwasser, F.; Panis, Y.; Soubrane, O.; Weill, B.; Batteux, F. Controlling tumor growth by modulating endogenous production of reactive oxygen species. *Cancer Res.* **2005**, *65*, 948–956.
- (10) Alexandre, J.; Batteux, F.; Nicco, C.; Chéreau, C.; Laurent, A.; Guillemin, L.; Weill, B.; Goldwasser, F. Accumulation of hydrogen peroxide is an early and crucial step for paclitaxel-induced cancer cell death both in vitro and in vivo. *Int. J. Cancer* **2006**, *119*, 41–48.
- (11) Ramanathan, B.; Jan, K. Y.; Chen, C. H.; Hour, T. C.; Yu, H. J.; Pu, Y. S. Resistance to paclitaxel is proportional to cellular total antioxidant capacity. *Cancer Res.* **2005**, *65*, 8455–8460.
- (12) Wenzel, U.; Nickel, A.; Daniel, H. alpha-Lipoic acid induces apoptosis in human colon cancer cells by increasing mitochondrial respiration with a concomitant O₂-* generation. *Apoptosis* **2005**, *10*, 359–368.
- (13) Fang, J.; Sawa, T.; Akaike, T.; Maeda, H. Tumor-targeted delivery of polyethylene glycol-conjugated D-amino acid oxidase for antitumor therapy via enzymatic generation of hydrogen peroxide. *Cancer Res.* **2002**, *62*, 3138–3143.
- (14) Wu, J. M.; Chen, Y.; Chen, J. C.; Lin, T. Y.; Tseng, S. H. Tetrandrine induces apoptosis and growth suppression of colon cancer cells in mice. *Cancer Lett.* **2010**, *287*, 187–195.
- (15) Kuo, P. L.; Lin, C. C. Tetrandrine-induced cell cycle arrest and apoptosis in HepG2 cells. *Life Sci.* **2003**, *73*, 243–252.
- (16) Jin, Q.; Kang, C.; Soh, Y.; Sohn, N. W.; Lee, J.; Cho, Y. H.; Baik, H. H.; Kang, I. Tetrandrine cytotoxicity and its dual effect on oxidative stress-induced apoptosis through modulating cellular redox states in Neuro 2a mouse neuroblastoma cells. *Life Sci.* **2002**, *71*, 2053–2066.
- (17) Janga, B. C.; Lima, K. J.; Paikb, J. H.; Choc, J. W.; Baeka, W. K. Tetrandrine-induced apoptosis is mediated by activation of caspases and PKC-d in U937 cells. *Biochem. Pharmacol.* **2004**, *67*, 1819–1829.
- (18) Wei, J.; Liu, B.; Wang, L.; Qian, X.; Ding, Y.; Yu, L. Synergistic interaction between tetrandrine and chemotherapeutic agents and influence of tetrandrine on chemotherapeutic agent-associated genes in human gastric cancer cell lines. *Cancer Chemother. Pharmacol.* **2007**, *60*, 703–711.
- (19) Li, X.; Zhen, D.; Lu, X.; Xu, H.; Shao, Y.; Xue, Q.; Hu, Y.; Liu, B.; Sun, W. Enhanced cytotoxicity and activation of ROS-dependent c-Jun NH2-terminal kinase and caspase-3 by low doses of tetrandrine-loaded nanoparticles in Lovo cells—a possible Trojan strategy against cancer. *Eur. J. Pharm. Biopharm.* **2010**, *75*, 334–340.
- (20) Li, X.; Li, R.; Qian, X.; Ding, Y.; Tu, Y.; Guo, R.; Hu, Y.; Jiang, X.; Guo, W.; Liu, B. Superior antitumor efficiency of cisplatin-loaded nanoparticles by intratumoral delivery with decreased tumor metabolism rate. *Eur. J. Pharm. Biopharm.* **2008**, *70*, 726–734.
- (21) Chou, T. C.; Talalay, P. Quantitative analysis of dose–effect relationships: the combined effects of multiple drugs or enzyme inhibitors. *Adv. Enzyme Regul.* **1984**, *22*, 27–55.
- (22) Mosmann, T. Rapid colorimetric assay for cellular growth and survival: application to proliferation and cytotoxicity assays. *J. Immunol. Methods* **1983**, *65*, 55–63.
- (23) Shao, J.; Zheng, D.; Jiang, Z.; Xu, H.; Hu, Y.; Li, X.; Lu, X. Curcumin delivery by methoxy polyethylene glycol-poly(caprolactone) nanoparticles inhibits the growth of C6 glioma cells. *Acta. Biochim. Biophys. Sin. (Shanghai)* **2011**, *43*, 267–274.
- (24) Shao, J.; Li, X.; Lu, X.; Jiang, C.; Hu, Y.; Li, Q.; You, Y.; Fu, Z. Enhanced growth inhibition effect of resveratrol incorporated into biodegradable nanoparticles against glioma cells is mediated by the induction of intracellular reactive oxygen species levels. *Colloids Surf., B* **2009**, *72*, 40–47.
- (25) Kirshner, J. R.; He, S.; Balasubramanyam, V.; Kepros, J.; Yang, C. Y.; Zhang, M.; Du, Z.; Barsoum, J.; Bertin, J. Elesclomol induces cancer cell apoptosis through oxidative stress. *Mol. Cancer Ther.* **2008**, *7*, 2319–2327.
- (26) Vobořilová, J.; Němcová-Fürstová, V.; Neubauerová, J.; Ojima, I.; Zandari, I.; Gut, I.; Kovář, J. Cell death induced by novel fluorinated taxanes in drug-sensitive and drug-resistant cancer cells. *Invest. New Drugs* **2011**, *29*, 411–423.
- (27) Xu, R.; Nakano, K.; Iwasaki, H.; Kumagai, M.; Wakabayashi, R.; Yamasaki, A.; Suzuki, H.; Mibu, R.; Onishi, H.; Katano, M. Dual blockade of phosphatidylinositol 3'-kinase and mitogen-activated protein kinase pathways overcomes paclitaxel-resistance in colorectal cancer. *Cancer Lett.* **2011**, *306*, 151–160.
- (28) Szanto, A.; Bogner, Z.; Szigeti, A.; Szabo, A.; Farkas, L.; Gallyas, F. Jr. Critical role of bad phosphorylation by Akt in cytostatic resistance of human bladder cancer cells. *Anticancer Res.* **2009**, *29*, 159–164.
- (29) Kim, S. H.; Juhnn, Y. S.; Song, Y. S. Akt involvement in paclitaxel chemoresistance of human ovarian cancer cells. *Ann. N.Y. Acad. Sci.* **2007**, *1095*, 82–89.
- (30) Mabuchi, S.; Ohmichi, M.; Kimura, A.; Hisamoto, K.; Hayakawa, J.; Nishio, Y.; Adachi, K.; Takahashi, K.; Arimoto-Ishida, E.; Nakatsuji, Y.; Tasaka, K.; Murata, Y. Inhibition of phosphorylation of BAD and Raf-1 by Akt sensitizes human ovarian cancer cells to paclitaxel. *J. Biol. Chem.* **2002**, *277*, 33490–33500.
- (31) Wang, Y. F.; Chen, C. Y.; Chung, S. F.; Chiou, Y. H.; Lo, H. R. Involvement of oxidative stress and caspase activation in paclitaxel-induced apoptosis of primary effusion lymphoma cells. *Cancer Chemother. Pharmacol.* **2004**, *54*, 322–330.
- (32) Wang, L. G.; Liu, X. M.; Kreis, W.; Budman, D. R. The effect of antimicrotubule agents on signal transduction pathways of apoptosis: a review. *Cancer Chemother. Pharmacol.* **1999**, *44*, 355–361.